Co-pyrolysis of torrefied biomass and coal: Effect of pressure on synergistic reactions

Saartjie M Gouws, Marion Carrier, John R Bunt, Hein W J P Neomagus

Co-pyrolysis of torrefied biomass and coal: Effect of pressure on synergistic reactions

Saartjie M. Gouws [a], Marion Carrier [b], John R. Bunt [a,*], Hein W.J.P. Neomagus [a]

[a] Centre of Excellence in Carbon-based Fuels, School of Chemical and Minerals Engineering, North-West University, Potchefstroom, 2520, South Africa
[b] RAPSODEE, CNRS UMR 5203, Université de Toulouse, IMT Mines Albi, Campus Jarlard, 81013 Albi CT Cedex 09, France

Keywords:
Co-pyrolysis
Biomass
Torrefaction
Pressure
Secondary reactions
Synergistic reactions

The co-utilization of torrefied biomass and coal in thermochemical conversion technologies is an attractive process for the transition to green energy and chemicals. The main advantage of this process is the production of high quality oil products (closer resembling crude-oil) via synergistic interaction of primary products from the two feedstocks. These synergistic reactions often involve secondary reactions, which are promoted at high pressures. This paper reports quantitative results on the extent of synergistic reactions and the role of pressure on these reactions during co-pyrolysis of torrefied biomass and coal. Torrefied biomass was produced at 280 °C in a pilot rotary kiln and subsequently both pyrolysis and co-pyrolysis of torrefied biomass and coal was investigated in a fixed bed reactor (heating rate 7 °C/min) at temperatures of 400–600 °C and pressures of 1, 15 and 30 bar. The results show that the prior removal of hemicellulose during torrefaction maximized the potential of hydrogen transfer from cellulose/lignin-derived products to depolymerized coal fragments. Furthermore, the dehydration and condensation reactions of depolymerized fragments were suppressed during co-pyrolysis in favour of synergistic reactions between the fragments. These reactions occurred predominantly in the molten/liquid phase and their rates could be indirectly controlled by pressure (through changing the evaporation rate), resulting in substantial changes in product distribution. In the presence of coal and its released vapours, the methoxyphenols (guaiacols) and furanics yields were significantly enhanced (positive deviation >54% and >40%, respectively, compared to additive predictions), whereas the phenol yields were inhibited (negative deviation >20%); suggesting the inhibition of demethoxylation reactions in the presence of coal depolymerized fragments. To date no studies have reported the molten phase synergistic reaction pathways occurring during co-pyrolysis of torrefied biomass and coal. Based on the findings in this paper, reaction pathways were proposed for these molten phase synergistic reactions.

1. Introduction

Thermochemical conversion technologies play an important role in the global production of both energy and chemicals [1]. The co-utilization of biomass and coal in existing coal-based conversion technologies has received increasing interest for its ability to reduce the dependence on fossil fuels and the production of higher quality products [2]. Co-pyrolysis is the first step in any coal and biomass thermochemical conversion technology and is also a feasible stand-alone technology for bio-oil/biochar production [6]. Industrial applications of fast pyrolysis include the BTG group's rotating cone reactor (RCR) and the Ensyn fluidized bed reactor (RTP®) [7]. Another industrial application of slow pyrolysis is as the primary step in fixed bed coal-to-liquid (CTL) gasification technology such as the commercial fixed bed dry bottom gasifier (FBDB™) [8]. An important feature of this industrial fixed bed gasifier is that it is operated at high pressures [9], therefore a need exists to study the co-pyrolysis process at these conditions.

The fuel properties of biomass as a feedstock (high moisture content, low energy density and high O/C ratio) lead to various operational challenges [3]. Torrefaction is considered to be one of the most

Abbreviations: ADF, acid detergent fibre; ADL, acid detergent lignin; BTX's, Benzene/Toluene/Xylene; d.a.f., dry ash free basis; FBDB, fixed bed dry bottom; MED, mass energy density; MS, mass spectrometer; NDF, neutral detergent fibre; PAH's, polyaromatic hydrocarbons; RCR, rotating cone reactor; RTP, rapid thermal processing; SAPPI, South African pulp and paper industries.

promising pre-treatment methods for upgrading biomass fuel properties to become more similar to coal [4]. The interest in the field of co-utilizing torrefied biomass and coal in co-pyrolysis technologies is illustrated by a recent review on the fundamental and engineering advantages of this process [5].

The attraction of the co-pyrolysis process lies not merely in its ability to reduce the carbon footprint of the overall process, but also in the potential of producing higher quality oil (composition closer resembling crude-oil) due to synergistic reactions [2]. These synergistic reactions between feedstocks often involve secondary reactions, the extent of which increases at higher pressures [10]. Therefore, the control of pressure is crucial to favour the extent of synergies during co-pyrolysis. Numerous co-pyrolysis studies of raw biomass and coal at atmospheric pressure are available [11–14], but only a few authors have studied the process at high pressure [15,16]. Aboyade et al. [15] used a factorial experimental design to investigate the effects of temperature, pressure and blend ratio on the yields and composition of co-pyrolysis products and concluded that no synergy was evident between the lumped solid, liquid and gas products, although significant deviations were reported for the oil composition. Collot et al. [16] reported that neither intimate contact between particles in a fixed bed nor segregation in a fluidized bed resulted in significant synergies, although deviations in the oil composition were apparent. The pressure was generally reported to have a negative effect on the oil yield and this was attributed to secondary reactions; however, the effect of pressure on the extent of the synergistic reactions, especially on secondary reactions, was not reported and no details on those reaction pathways occurring between feedstocks were provided. Furthermore, these studies were performed using raw biomass and coal blends, and no literature is available for the use of torrefied material, which could significantly alter secondary/synergistic reaction pathways during co-pyrolysis.

Secondary pyrolysis reactions often include homogeneous (gas-gas) and heterogeneous (gas-char) reactions of the primary volatiles [17]. Homogeneous (cracking) reactions occur when primary volatiles (upon leaving the pyrolyzing particle) decompose further in the gas-phase and produce low molecular weight volatiles and non-condensable gases, whereas heterogeneous (polymerization/condensation) reactions proceed when primary volatiles come into contact with solid particles (char/ash/catalysts) and produce secondary char, CO_2 and water [18]. The extent of these reactions is known to depend, among others, on the vapour residence time, temperature, nature of the solid surfaces, reactor configuration and concentration of the primary vapours [18–21]. He et al. [22] critically reviewed secondary reactions during biomass gasification and other authors have investigated these reactions during pyrolysis of woody biomass at atmospheric pressures [18,20,23]. Morf et al. [20] suggested that the influence of homogeneous secondary reactions only became significant at temperatures above 650 °C in a fixed bed reactor. In contrast, Boroson et al. [23] showed that, for a fixed bed reactor, those reactions cannot be ignored at lower temperatures (500 °C) and Hoekstra et al. [18] reported a significant effect of secondary reactions on product yields and composition at temperatures of 400–550 °C in a fluidized bed reactor. They observed that an increase in vapour residence time increased the extent of homogeneous secondary reactions which resulted in a change in the volatile yields and composition. Primary aldehydes were cracked and produced CO, whereas guaiacols were cracked to form phenols. Furthermore, they reported that the presence of mineral matter in the biomass/char matrix significantly enhanced the number of heterogeneous charring/polymerization secondary reactions. Anca-Couce et al. [21] demonstrated how the extent of heterogeneous secondary reactions affected char reactivity in a fixed bed reactor at 500 °C. It was suggested that when the extent of heterogeneous secondary reactions increased, they played a significant role in the deactivation of primary active sites (through the deposition of secondary char) and reduced the overall char reactivity.

Apart from homogeneous and heterogeneous secondary reactions, molten pyrolysis products can also break down in the liquid phase. Mettler et al. [24] reported that levoglucosan undergoes secondary breakdown in the pyrolysis liquid intermediate (to form pyrans and light oxygenates) and proposed a reaction pathway suggesting intermolecular hydrogen transfer. For coal pyrolysis, the significant role of hydrogen transfer for the cleavage of strong bonds and the prevention of retrogressive reactions was demonstrated by McMillen and Malhotra [25]. These secondary liquid phase reactions involving hydrogen transfer may be presumptive evidence to understanding why significant deviations in specifically oil composition are generally reported for co-pyrolysis studies. To the knowledge of the authors, no studies have reported on the reaction pathways of liquid phase synergistic reactions occurring between torrefied biomass and coal during co-pyrolysis. The novelty of this paper is twofold: it is the first to report on the composition of condensates derived during co-pyrolysis of specifically torrefied biomass and coal. Secondly, by systematically investigating the influence of pressure on the deviation from additive predictions of grouped and individual product yields, reaction pathways for synergistic reactions occurring in the molten phase have been proposed.

2. Material and methods

2.1. Raw materials

The coal sample used in this work was a South African medium rank C bituminous coal. The bulk coal sample was crushed using a hammer mill (TRF-70) to a particle size of <8 mm and a smaller representative sample was obtained through cone and quartering. This sample was then further crushed using a ball mill to a particle size range of 37–74 μm and stored under nitrogen in airtight containers. The biomass sample was a mixture of softwood (Pine) and hardwood (Eucalyptus) chips (<8 mm) obtained as a waste product from the Ngodwana Mill of the South African Pulp and Paper Industries (SAPPI). The bulk sample was air dried for 1 week before a smaller representative sample was obtained by cone and quartering. This sample was then crushed using a hammer mill (TRF-70) and sieved to a particle size range of 37–74 μm using no. 200 and no. 400 sieves.

2.2. Torrefaction and characterization

Prior to torrefaction, a TG/DTG analysis was performed on the raw biomass (shown in the Supplementary Data - Figs. S1 and S2, respectively) to determine the optimal temperature for torrefaction. From these results, the temperature of 280 °C was identified as the temperature of maximum degradation of the hemicelluloses in the biomass and was therefore selected. Furthermore, two different criteria were used to evaluate the efficiency of the torrefaction process: Mass energy density (MED) [26] and O/C molar ratio [27,28]. The MED allows the upgrade in fuel energy content to be analysed with respect to the mass loss during torrefaction [29]. A MED >1 indicates an upgrade in the fuel properties of the material [30].

A pilot plant scale torrefaction rig consisting of a continuous rotary kiln reactor (diameter of 0.3 m and a length of 2 m) was used to produce the torrefied material. The bulk sample of raw biomass (<8 mm) was fed to the reactor at a feed rate of 20 kg/h and the residence time of the material was 60 min. Nitrogen (purity > 99.999%, Afrox) with a gas flow rate of 4 L_n/min was used to ensure an inert atmosphere inside the reactor. After bulk torrefaction, a representative sample was obtained through cone and quartering and crushed using a hammer mill to a particle size of 37–74 μm.

Elemental and X-ray fluorescence (XRF) analyses of the raw/torrefied biomass and coal (Table 1) were performed at Bureau Veritas Testing and Inspectors South Africa. The compositional analysis for the raw/torrefied biomass (Table 2) was carried out at ARC-Analytical services, Republic of South Africa by determining neutral detergent fibre (NDF), acid detergent fibre (ADF) and acid detergent lignin (ADL).

A mass yield of 67% was determined after bulk torrefaction of the

Table 1
Proximate and ultimate analyses of raw/torrefied biomass and coal.

	Standard method	Raw biomass	Torrefied biomass	Coal
Proximate analysis in wt% (d.b.[a])				
Volatile matter	ISO 562:2010	82.9	70.4	26.4
Ash	ISO 1171:2010	1.5	2.0	16.4
Fixed carbon	by difference	15.6	27.5	57.3
Ultimate analysis in wt% (d.a.f.[b])				
Carbon	ASTM D5373	54.4	59.5	84.0
Hydrogen	ASTM D5373	5.8	5.7	4.2
Nitrogen	ASTM D5373	0.1	0.1	2.0
Sulfur	ASTM D4239	0.1	0.1	1.0
Oxygen	by difference	39.6	34.7	8.8
Gross Calorific Value (MJ/kg)	ISO 1928:2009	17.8	21.9	26.2
O/C molar ratio		0.5	0.4	0.1
H/C molar ratio		1.3	1.1	0.6
XRF analysis in wt% (d.b.)	ASTM D4326 XRF			
Al_2O_3		6.6	7.3	25.6
CaO		9.7	10.2	3.9
Cr_2O_3		0.6	0.5	0.1
Fe_2O_3		11.0	9.7	2.9
K_2O		4.2	4.5	1.0
MgO		2.3	2.3	1.6
MnO		0.7	0.7	0.0
Na_2O		0.9	0.7	0.1
P_2O_5		1.9	2.1	0.7
SiO_2		50.4	46.7	59.2
TiO_2		0.3	0.2	1.5
V_2O_5		n.d.[c]	n.d.	0.0
ZrO_2		0.1	0.1	0.1
BaO		0.1	0.1	0.1
SrO		0.1	0.1	0.3
ZnO		0.1	0.1	0.0
SO_3		11.3	15.3	2.9

[a] d.b. – dry basis.
[b] d.a.f. – dry ash free basis.
[c] n.d. – not detected.

Table 2
Compositional analysis of raw biomass in wt% (g/100 g feedstock air dried) and torrefied biomass in wt% (g/100 g raw biomass air dried).

	Raw biomass	Torrefied biomass
Hemicelluloses	10.4	0.9
Cellulose	51.2	38.9
Lignin	22.2	23.5
Non-structural carbohydrates	3.1	0.5
Ash	1.3	1.3
Moisture	11.8	1.9

raw material through weighing of the final and initial sample masses on an industrial scale (BT model, BAYKON Inc.). An energy yield of 82% was determined from the difference in the calorific values of the raw and torrefied materials, resulting in an MED of 1.2. As seen in Table 1, the O/C molar ratio of the biomass decreased from 0.5 to 0.4 after torrefaction and therefore the torrefied material met both criteria.

2.3. Pyrolysis experiments

The pyrolysis experimental rig (Fig. 1) consisted of a reactor section, product capture and an analysis section. The reactor section was comprised of a vertical 800 mm 1 ½" ASTM 316 Grade stainless steel tube (OD: 38.1 mm, ID: 31.3 mm) and a stainless-steel mesh (aperture size: 25 μm) which was installed halfway into the tube. For each run, 20 g of sample was loaded onto this mesh to form a fixed bed. Argon (purity > 99.999%, Afrox) was introduced at the bottom of the reactor and the flow rate regulated between 0.2 and 6.0 L_n/min using a mass flow controller (EL-FLOW, Bronkhorst High Tech®) to obtain a constant gas velocity at different reactor pressures (1–30 bar). The reactor pressure was controlled downstream by a thermal back pressure regulator (TBPR) from Equilibar. Once the sample was loaded, the reactor was purged with Argon for 5 min and then pressurized. Upon reaching isobaric conditions, the sample was heated at 7 °C/min to temperatures ranging from 400° to 600°C using an electric vertical split-tube furnace. Upon reaching the target temperature, the solid was quenched with argon gas and subsequently removed. The residence time of pyrolysis varied between 53.6 and 82.1 min for the temperature range of 400–600 °C. Two K-type thermocouples were used to monitor the bed temperature and the temperature at the outlet of the reactor, respectively. The outlet temperature was kept at 300–350 °C by using a ceramic insulation box with an electric heat source and filter (SS-4TF-140, Swagelok) to prevent condensation of volatiles in the thermal back pressure regulator.

The volatile products were swept out of the reactor to a condenser system which consisted of 3 ice-cooled condensers followed by an acetone (purity 99.5%, Glassworld) liquid trap. The condensers were weighed on a balance (M5-M1003i, BEL Engineering) prior to and after each run to determine the total condensable product yield (the aqueous and organic phases were not separated). The water content of the condensable products was determined by Karl Fischer titration (ASTM 6304, using an Aquastar® CombiTitrant). The non-condensable gases were sent to an online mass spectrometer (Cirrus 2™ Quadrupole Mass Spectrometer, Micromeritics Instruments), which was operated in scan mode and a range of 1–49 *m/z*. Data was acquired every four seconds on the Process Eye Professional 8.0 software. A calibration was obtained for the quantitative measurement of four major pyrolysis gases (CO, CO_2, H_2 and CH_4) using analytically certified gas mixtures from Afrox and the cumulative yield of the gases was obtained by integration of the concentration curves. Prior to the experiments, a step-test was conducted at three different pressures (1, 15 and 30 bar) to determine the time interval for the non-condensable gas products to travel through the condensers and be detected by the online mass spectrometer (MS). The gas production curves from the online MS were then adjusted with this time. The F(t)-curves obtained from the step-test are shown in the Supplementary Data (Fig. S3). Furthermore, the solid remaining after each run was collected and weighed (M5-M1003i balance, BEL Engineering) to determine the char yield. A mass balance was determined for each run and product yields corresponded to >93% of the initial sample mass. The repeatability of the system was also tested and the average experimental uncertainty was determined to be 7% (Supplementary Data Section S3).

2.4. GC-MS analysis of condensables

The GC-MS analysis of the condensable products was performed at Central Analytical Facilities (Stellenbosch, South Africa). Separation was performed on a gas chromatograph (6890N, Agilent technologies network) coupled to an Agilent technologies inert XL EI/CI Mass Selective Detector (MSD) (5975B, Agilent technologies Inc., Palo Alto, CA).

For analysis of the torrefied bio-oil samples, a ZB-Waxplus capillary column (30 m × 0.25 mm × 0.25 μm) from Phenomenex was used. Helium (purity > 99.999%, Afrox) was used as the carrier gas at a flow rate of 1.0 mL/min. The injector temperature was maintained at 250 °C where the injection was performed in split-less mode. The oven temperature was programmed as follows: 60 °C for 3 min and ramped at a rate of 10 °C/min until 280 °C and held for 3 min and finally ramped at a rate of 20 °C/min until 320 °C and held for 4 min. The MS was operated in full scan mode and the source and quadrupole temperatures were maintained at 230 and 150 °C, respectively. The transfer line temperature was maintained at 250 °C. The mass spectrometer was operated under electron impact (EI) mode at an ionization energy of 70 eV, scanning from 40 to 650 *m/z*. The compounds were identified using both WILEY 275 and NIST 95 libraries.

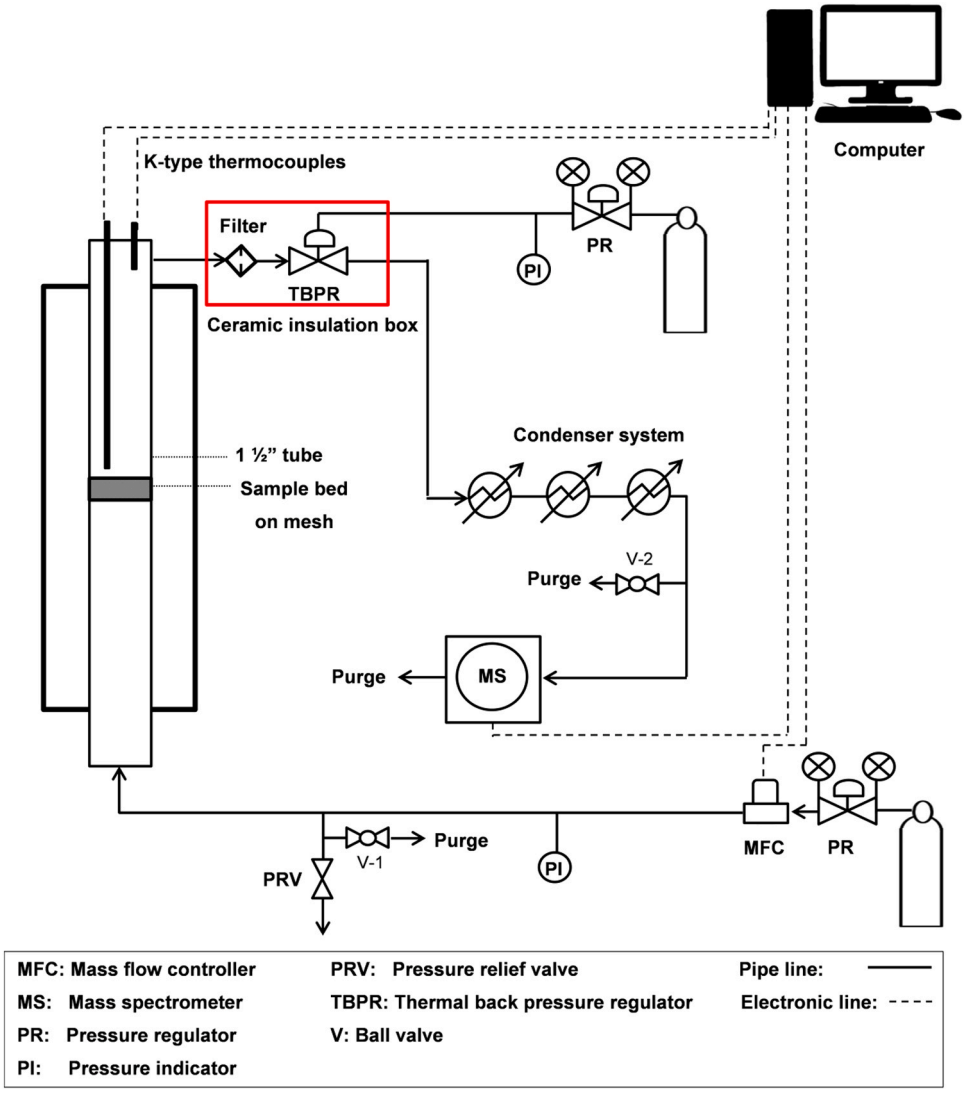

Fig. 1. High pressure pyrolysis rig.

For the quantification of levoglucosan, a 30 m x 0.25 mm× 0.10 μm capillary column (VF-5ht UltiMetal, Agilent) was used. Helium (purity > 99.999%, Afrox) at a flowrate of 1.0 mL/min and a constant pressure of 45.49 kPa was used as carrier gas using a split ratio of 10:1. The injector temperature was 250 °C and the injector volume was 1 μL. The temperature program of the GC oven was as follows: 45 °C for 8 min, ramped at 2 °C/min to 100 °C and then at 7 °C/min to 162 °C and held for 5 min. It was then ramped at 7 °C/min to 300 °C and finally ramped at 20 °C/min to 350 °C. The MS was operated in scan mode and the mass spectra were obtained between 29 and 600 *m/z*. The temperature of the MS source and quadrupole was 230 °C and 150 °C, respectively.

For the analysis of the coal derived oil samples, a DB-FFAP (60 m x 0.32 mm × 0.50 μm) capillary column (Phenomenex) was used in the GC/MS system. Helium (purity > 99.999%, Afrox) was used as the carrier gas at a flow rate of 2.0 mL/min. The oven temperature was programmed as follows: 40 °C for 10 min and ramped at a rate of 15 °C/min until 250 °C and held for 4 min. All other parameters were the same as described above. For the 26 components, a 7-point calibration curve with $R^2 > 0.99$ was obtained using standards supplied by Sigma-Aldrich with a purity of >99.8%. 2-Octanol was used as the internal standard and acetone as the solvent (both with a purity of > 99.8%).

3. Results and discussion

3.1. Pyrolysis of single feedstocks: role of pressure

3.1.1. Torrefied biomass

In general, an increase in pressure (from 1 to 30 bar at different temperatures, 400–600 °C) showed a negative effect on oil yields (−6 wt %) and a positive effect on gas (+9 wt%), pyrolytic water (+2 wt%) and char yields (+2 wt%) (Fig. 2), which is consistent with general trends reported in literature [31,32]. The observation of main pyrolysis gases yields (Fig. 3) and their release rates (Fig. 4) has allowed the identification of different reaction pathways occurring during pyrolysis of torrefied biomass. The curves depict a 2-stage gas release process: a first stage which occurred between 300 and 400 °C and a second stage between 400 and 600 °C. In the first stage, the production of CO and CO_2 (Figs. 4a and 4b) was dominant due to decarbonylation and decarboxylation of the holocellulose polymers, whereas production of CH_4 (Fig. 4c) was attributed to demethylation of lignin polymers through cracking of methoxy groups [33]. The production of H_2 (Fig. 4d) was dominant in the second stage due to the rearrangement of the aromatic rings into a polycyclic char structure as well as the secondary repolymerization reactions [33]. The observed increase in water yields during this second stage (Fig. 2c) was attributed to polycondensation reactions. These results therefore suggest a competitive pattern of two kinds of

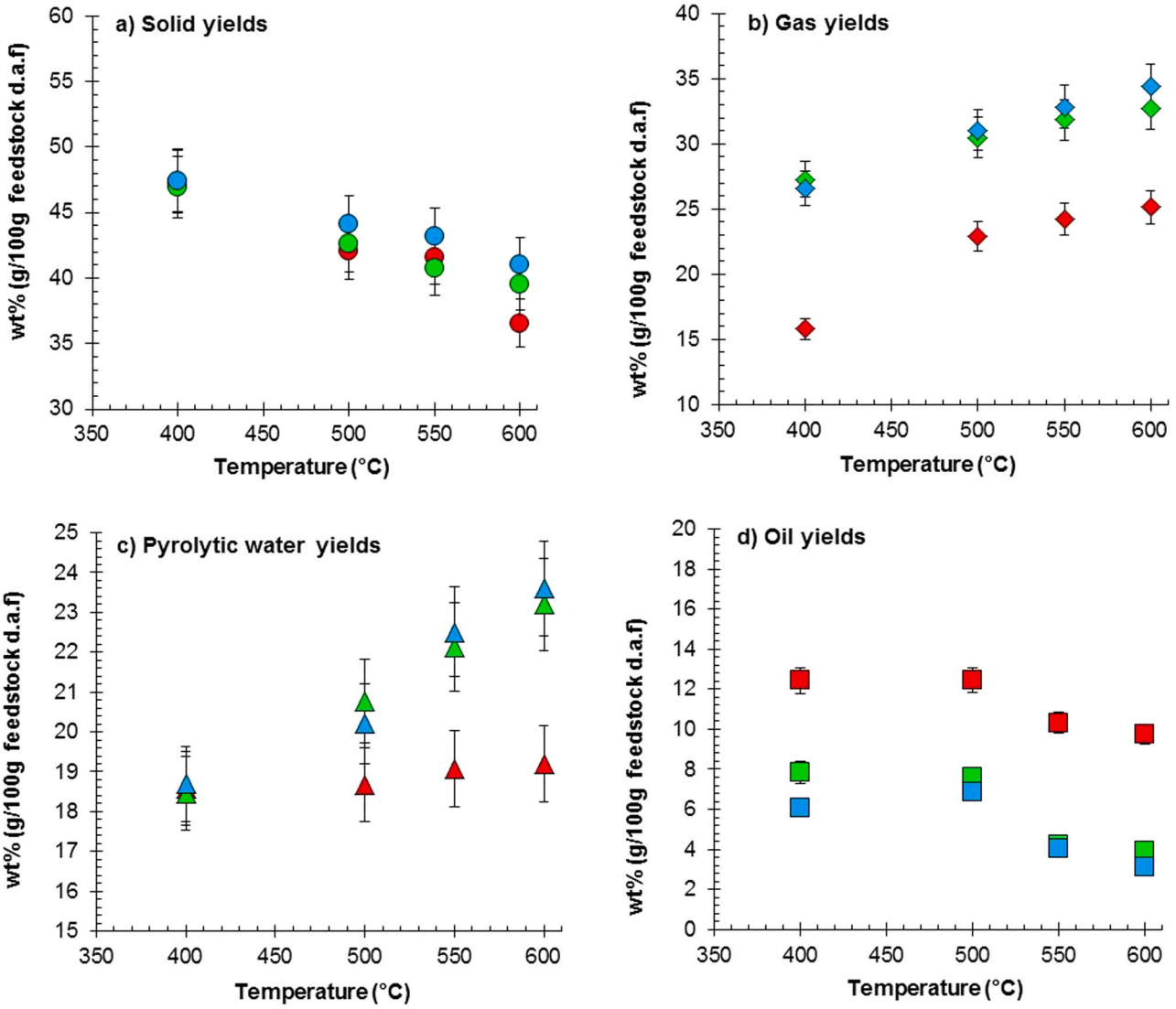

Fig. 2. The effect of pyrolysis pressure and temperature on a) solid residue yields (● 1 bar), (● 15 bar), (● 30 bar), b) gas yields (◆ 1 bar), (◆ 15 bar), (◆ 30 bar), c) pyrolytic water yields (▲ 1 bar), (▲ 15 bar), (▲ 30 bar) and d) oil yields (■ 1 bar), (■ 15 bar), (■ 30 bar) of torrefied biomass.

reaction pathways for pyrolysis of torrefied biomass: Depolymerization/volatilization, which results in the production of low molecular weight oxygenates and repolymerization/polycondensation of high molecular weight components to produce char, water and non-condensable gases [34]. The pressure significantly enhanced the rates of these different reactions, which is evident from the increase in the gas release rates with increasing pressure for both stages (Fig. 4) as well as the increase in the water and char yields at high pressures (Fig. 2a and c).

The oxygen release rate at different pressures (Fig. 5) clearly demonstrates the increase in the rate of deoxygenation at higher pressures through the release of CO and CO_2. Although deoxygenation occurred through the removal of both CO and CO_2 groups, the effect of pressure on the release rate of CO_2 was more significant compared to CO. CO has previously been reported as a major product of homogeneous (vapour phase) cracking reactions, whereas CO_2 and H_2 are important products formed during repolymerization/secondary charring [18]. As shown in Fig. 3, the cumulative yields of CO_2 and H_2 both increased almost 1.6 times when the pressure was increased from 1 to 30 bar at 600 °C. The CO_2 yields increased most significantly between 1 and 15 bar but showed an asymptote-like trend for a further increase in pressure. Similar trends were observed for the effect of pressure on the pyrolytic water and char yields (Figs. 2c and 2a). Pyrolytic water, char and CO_2 are all products of repolymerization/secondary charring reactions [18], which may explain why their yields showed similar trends. These results therefore suggest that pressure has a more significant effect on the secondary charring reactions compared to the secondary cracking reactions. This was further proven by the absence of any significant change in the gas yield when the flow rate of the sweep gas was doubled (Supplementary Data Tables S7-S8).

Previously, it has been reported that in comparison with raw wood, repolymerization reactions play a more significant role during pyrolysis of torrefied wood due to the physico-chemical changes in the biomass structure caused by torrefaction [35]. For example, the increase in microporosity of torrefied biomass could limit the diffusion of volatiles out of the particle, therefore favouring the recombination reactions within the pores of the particle [5]. Furthermore, during the torrefaction pre-treatment, dehydration is the dominant reaction mechanism leading to char formation and the removal of H and O [5]. This prior removal of water can significantly enhance the subsequent repolymerization reactions during pyrolysis of torrefied biomass. In addition, with the removal of hemicelluloses during torrefaction (Table 2), fewer of free

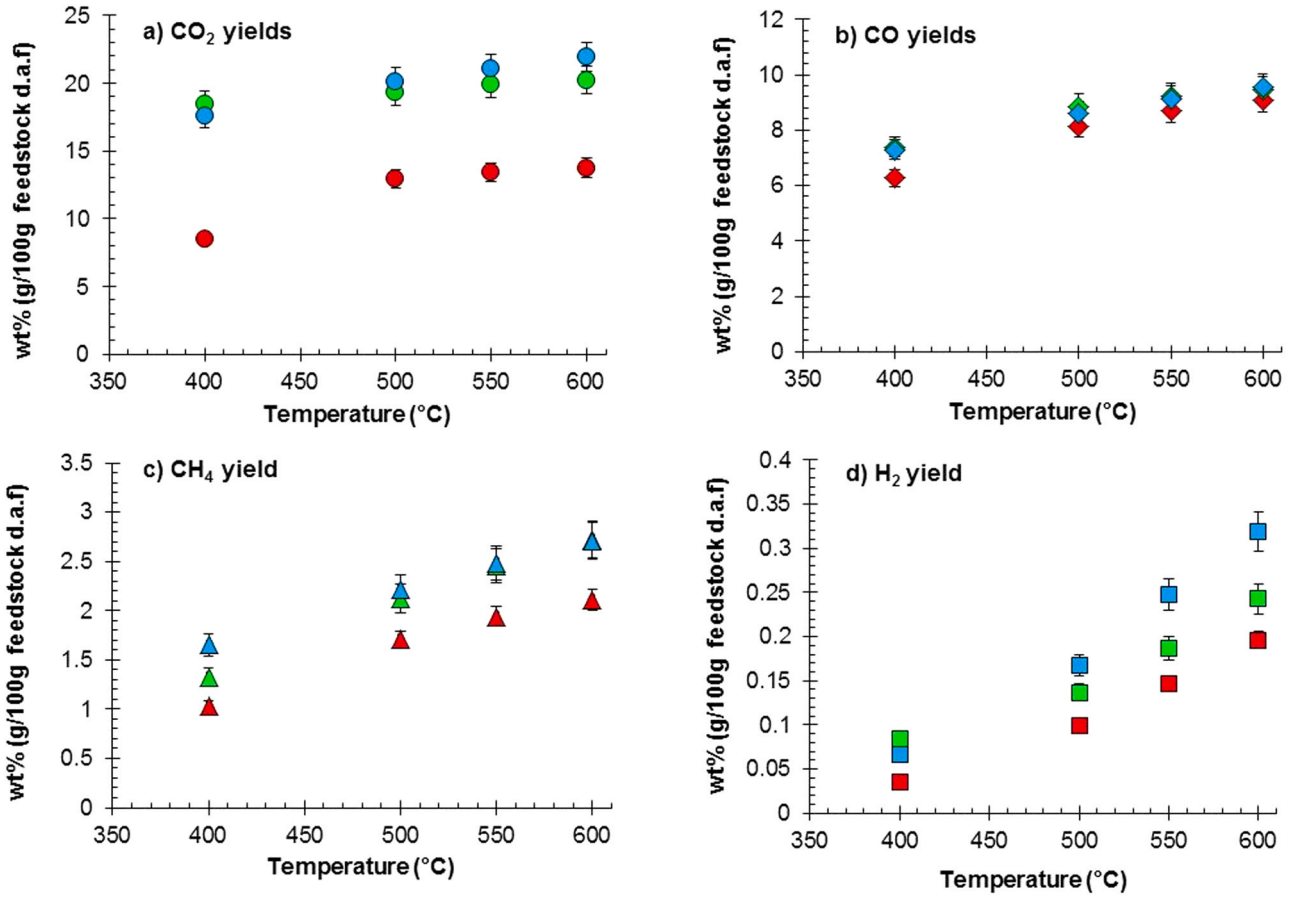

Fig. 3. The effect of pyrolysis pressure and temperature on a) CO_2 yields (● 1 bar), (● 15 bar), (● 30 bar), b) CO yields (◆ 1 bar), (◆ 15 bar), (◆ 30 bar), c) CH_4 yields (▲ 1 bar), (▲ 15 bar), (▲ 30 bar) and d) H_2 yields (■ 1 bar), (■ 15 bar), (■ 30 bar) of torrefied biomass.

radicals that are vigorously consumed during the volatilization of the lignin bio-polymer are available, thereby favouring repolymerization reaction pathways against volatilization pathways [36].

The effect of pressure on the reaction pathways during pyrolysis of torrefied biomass has been further investigated through trends in the yields of the main chemical family groups in the bio-oil (reported as wt% of dry oil) (Fig. 6). The yields of the individual components are provided in the Supplementary Data – Table S9. On average, the quantified components made up approximately 20 wt% of the pyrolysis oil, which is similar to values reported in literature for GC-MS analysis of bio-oils [37,38]. The yields of the main family groups at 1 bar are in the same range as the results reported by Konsomboon et al. [39] and Lyu et al. [37] for oil derived from torrefied wood at atmospheric pressure. An important benefit of using torrefied biomass as feedstock is that, compared to raw biomass, the pre-removal of hemicelluloses during torrefaction results in lower yields of water and organic acids/light oxygenates and increased sugar and phenol yields in the bio-oil (due to a relative increase in the cellulose and lignin content of torrefied biomass) [39]. As a result, the torrefied bio-oil is chemically more homogeneous with higher quantities of some key compounds (methoxyphenols and phenols), which is beneficial for subsequent upgrading of the oil [40].

The most significant effect of pressure on the oil composition was observed for the anhydrous sugar group (assumed to consist entirely of levoglucosan in this study). A significant drop in levoglucosan yield is observed from 1 to 15 bar (Fig. 6d). At 1 bar, the levoglucosan content of the oil was 3.7 wt%; however, it decreased sharply to 0.7 wt% when the pressure was increased to 15 bar. Levoglucosan is subject to three types of secondary reactions: (1) volatilization (decomposing into non-condensable gases in the vapour-phase), (2) repolymerization (char formation in the liquid intermediate) and (3) secondary breakdown through reaction with the liquid intermediate [24,41]. At higher pressures, the evaporation of levoglucosan into the vapour phase is supressed and therefore the reactions occurring in the liquid intermediate dominate under these conditions (polymerization and reaction with liquid intermediate). Moreover, the decrease in levoglucosan yield at high pressures was accompanied by an increase in char yield (Fig. 2a), supporting this hypothesis. Another indication of the increase in the rate of polymerization reactions of levoglucosan with pressure, is the increase in acid yield (a well-known by-product of polymerization [42]) at higher pressures. Furthermore, the reaction of the molten levoglucosan with the liquid intermediate was also enhanced at high pressures. These reactions involve elimination and cyclization, which are promoted through intermolecular hydrogen exchange between molecules in the liquid intermediate [24]. The rates of these reactions are, indirectly, a function of the liquid intermediate evaporation rate, which is a function of pressure [43]. Therefore, the rate of deoxygenation via elimination increased with pressure (Fig. 5).

The pressure also significantly affected the demethoxylation/demethylation rate. At 600 °C, the methoxyphenols decreased by almost 40%, whereas the phenols increased by 66% when the pressure increased from 1 to 30 bar. At lower pressure, a higher number of products resembling lignin's monomeric structures (e.g., 4-methylguaiacol, 4-ethylguaiacol and guaiacol) were present (Table S9). However, as the pressure was increased, the direct trend between the decrease in 'guaiacols' yield and the increase in 'phenols' (e.g., p-cresol, 4-ethylphenol and phenol) confirmed substantial demethoxylation reactions.

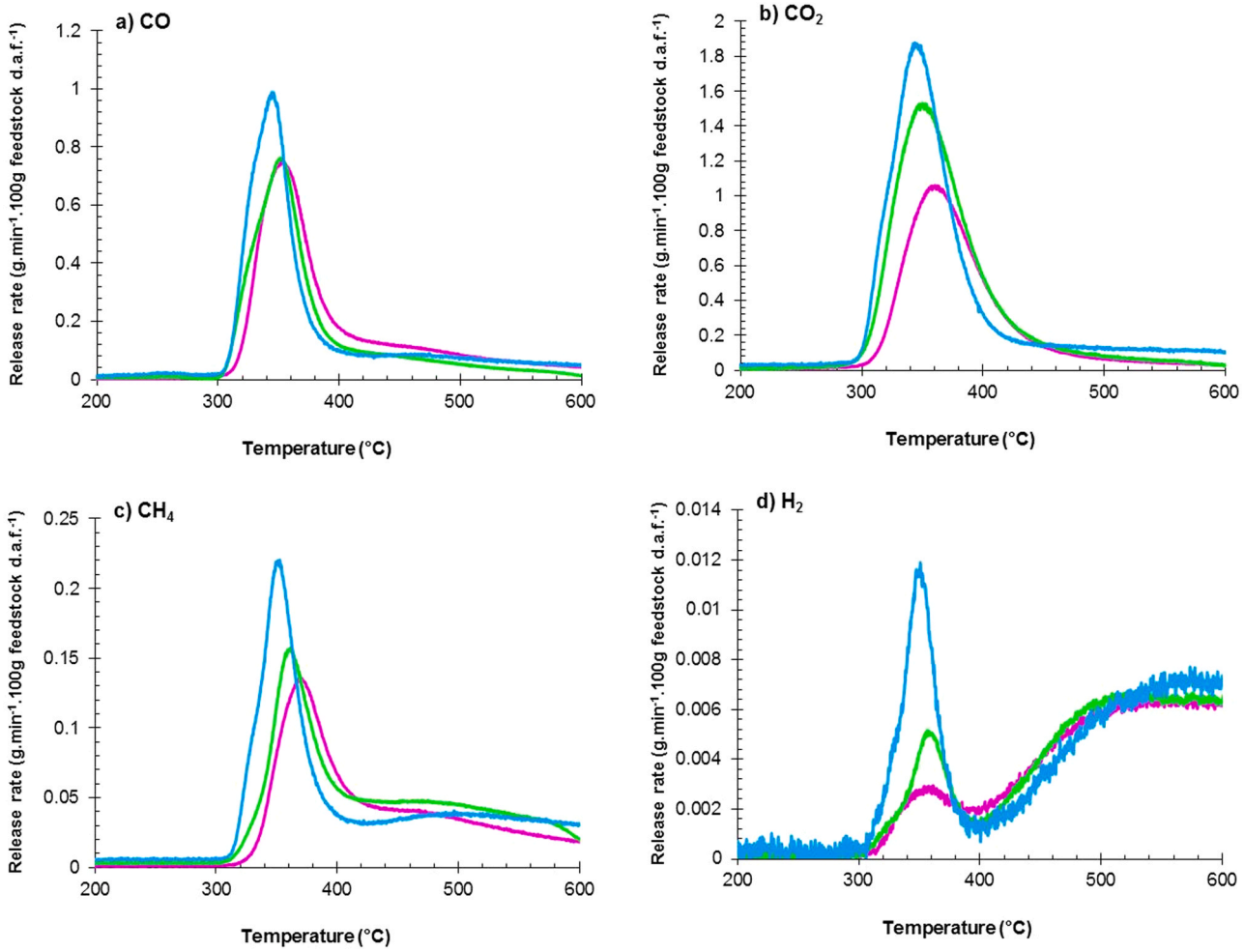

Fig. 4. The release rate of a) CO, b) CO_2, c) CH_4 and d) H_2 during pyrolysis of torrefied biomass at pressures of 1 bar (—), 15 bar (—) and 30 bar (—).

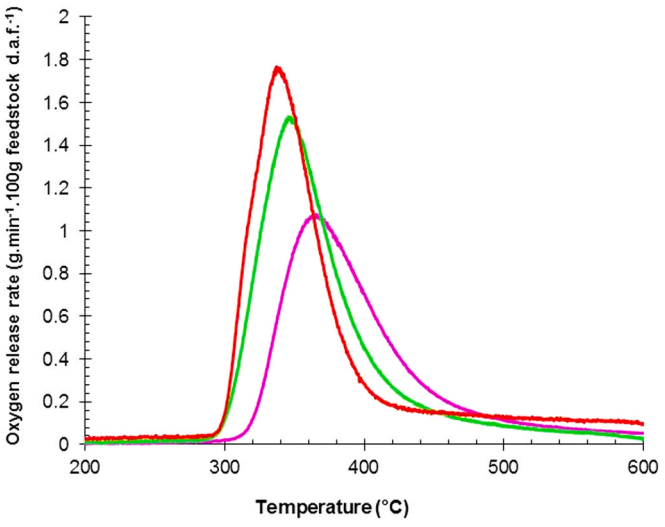

Fig. 5. The oxygen release rate during pyrolysis of torrefied biomass at pressures of 1 bar (—), 15 bar (—) and 30 bar (—).

Furthermore, the increase in the H_2 partial pressure with increasing reactor pressure could have promoted the deoxygenation of phenolic compounds to aromatics and polyaromatic hydrocarbons (PAH's) at higher pressures (Table S9).

To summarize, the reactor pressure is an indirect controlling factor for the promotion of different reaction pathways during pyrolysis of torrefied biomass. It plays a significant role in the deoxygenation of primary oxygenates by controlling the evaporation rate of the liquid intermediate and therefore the rate of secondary repolymerization. Furthermore, the pressure promotes secondary molten phase reactions by maximizing the residence time of depolymerized fragments in this phase.

3.1.2. Coal

The effect of pressure on lumped products (solid, liquid and gas) yields of coal pyrolysis: solid yields ranging between 79.0 and 86.9 wt% (d.a.f), liquid yields between 4.1 and 5.7 wt% (d.a.f) and gas yields between 5.1 and 13.2 wt% (d.a.f) (Fig. 7), agrees with results reported by other authors for fixed bed pyrolysis of South African bituminous coals [15,44]. In general, an increase in pressure resulted in a significant decrease in the oil yields, from 1.8 wt% to 0.8 wt% at 600 °C (Fig. 7d), and an increase in the gas and pyrolytic water yields, from 10.1 wt% to 13.3 wt% and 3.9–4.4 wt%, respectively (Fig. 7b-c).

The cumulative yield of major gases (Fig. 8) and their respective release rates (Fig. 9) indicate two stages of gas release: first stage between 300 and 400 °C where decarbonylation and decarboxylation reactions dominated to release CO and CO_2, followed by a second stage at 400–600 °C where all four major gases were produced. The first stage of gas release may be attributed to the scission of weak aliphatic-ether

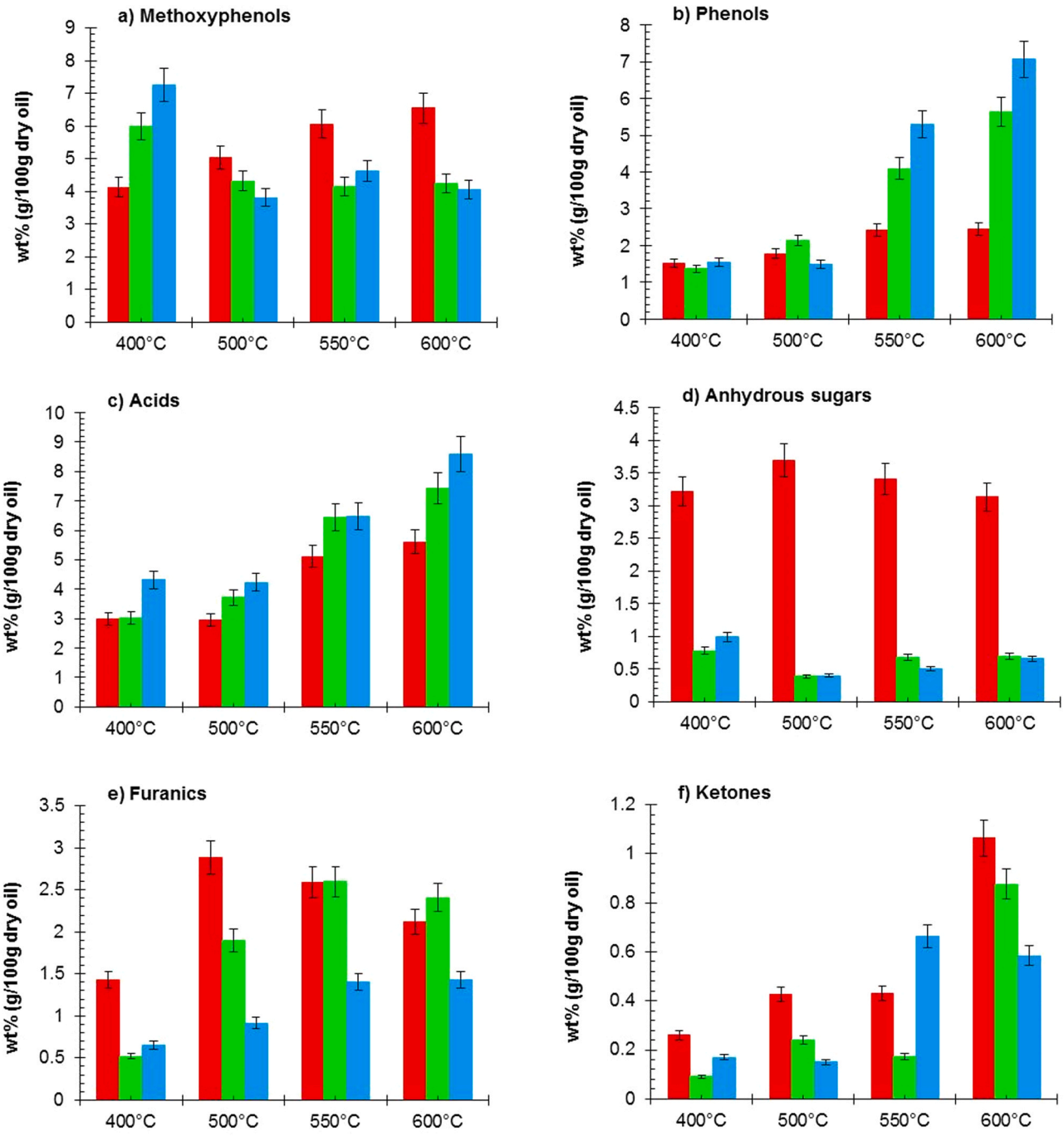

Fig. 6. Yields of a) methoxyphenols, b) phenols, c) acids, d) anhydrous sugars, e) furanics, and f) ketones during pyrolysis of torrefied biomass at pressures of 1 bar (■), 15 bar (■) and 30 bar (■).

bonds of small molecular side groups attached to the macromolecular network, whereas the second stage is related to depolymerization through rupture of the weaker bridges in the macromolecular network to release smaller fragments, which make up the metaplast (liquid intermediate) [45,46]. Two subsequent reaction pathways then occur at this stage: Repolymerization/cross-linking reactions of the metaplast and vaporization of lighter organic molecules [47].

The pressure significantly affected the release rate of gases in both stages (Fig. 9). For the first stage, the rates of deoxygenation reactions increased with pressure (Fig. 10). In the second stage, it was observed that the yields of CO_2 and CH_4 were more significantly affected by pressure compared to the CO yield. At 600 °C, CO_2 increased by almost 40% and CH_4 by 60% when the pressure increased from 1 to 30 bar, whereas the CO yield increased by 28%. CO_2 and CH_4 are indicative of cross-linking reactions of free radicals, whereas CO is associated with cracking reactions after vaporization [47]. At higher pressure, the evaporation rate of organic molecules from the metaplast decreased, promoting the cross-linking reactions pathway with the release of higher yields of CO_2 and CH_4 (Fig. 8a-c). At 600 °C, the polyaromatic hydrocarbons (PAHs) yields decreased by 30% when the pressure was increased from 1 to 30 bar (Table 3). This result is another indication of the dominance of the cross-linking reactions at high pressure [48]. The high yield of phenolic groups is attributed to the relatively low temperatures used for coal pyrolysis in this study [49].

The increase in the yield of phenolic groups with pressure (Table 3) indicates that there was an increase in the scission rate of O-containing

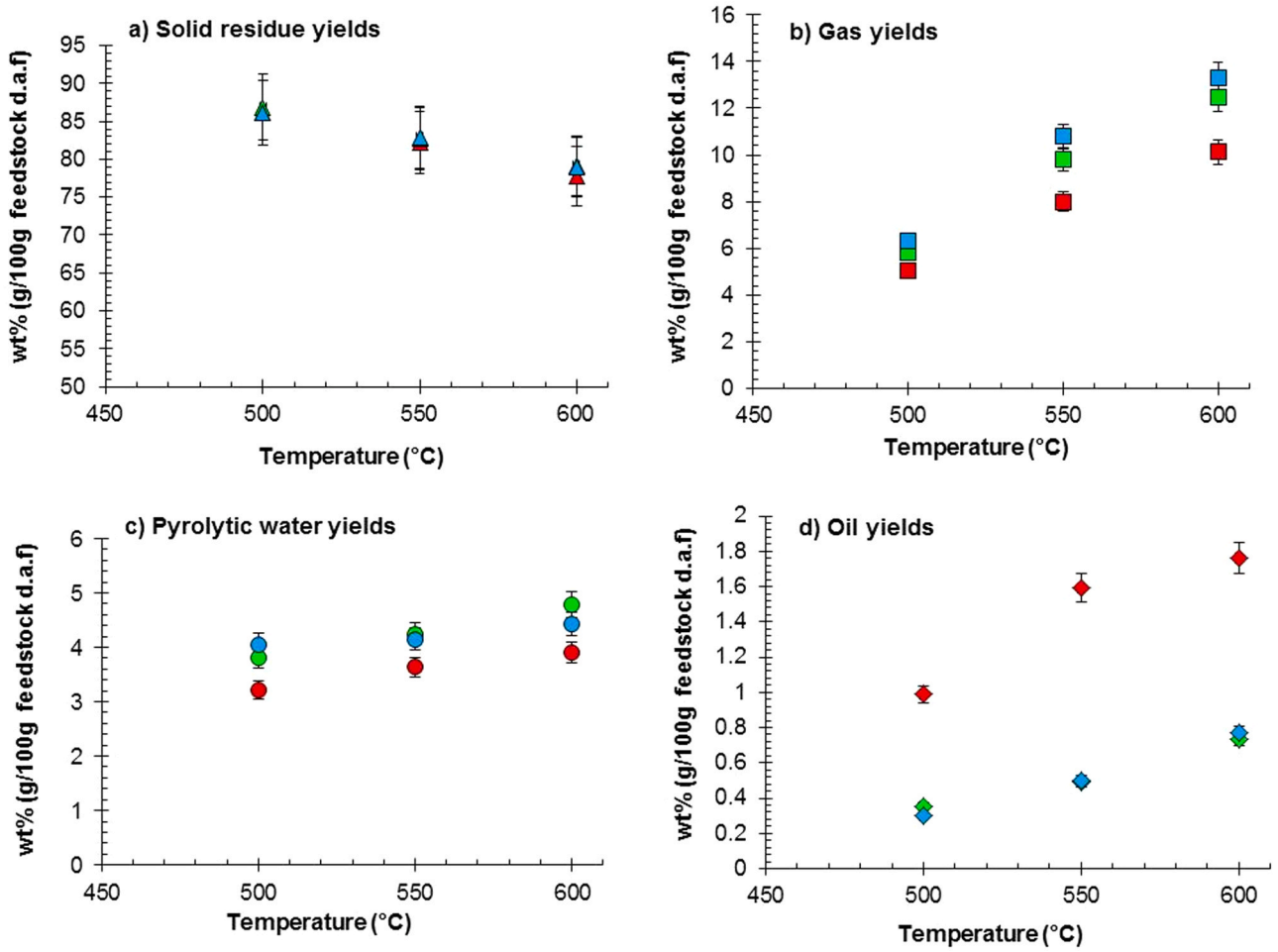

Fig. 7. The effect of pyrolysis pressure and temperature on a) solid residue yields (▲ 1 bar), (▲ 15 bar), (▲ 30 bar), b) gas yields (■ 1 bar), (■ 15 bar), (■ 30 bar), c) pyrolytic water yields (● 1 bar), (● 15 bar), (● 30 bar) and d) oil yields (◆ 1 bar), (◆ 15 bar), (◆ 30 bar) of coal.

ether bonds at high pressure [50]. Furthermore, the increase in (Benzene/Toluene/Xylene) BTX groups at higher pressure could be due to an increase in the secondary cyclization and dehydration of aliphatic compounds, which suggest the promotion of secondary vapour phase reactions at higher pressures [51]. According to Solomon et al. [32], the ratio of phenolics/BTX yield (Table 3) is a reliable indicator for the presence of secondary reactions where a ratio < 1 is required for the production of primary tar. In this study, the ratio is much larger than 1, which clearly indicates the importance of secondary reactions in fixed bed reactors. The same ratio was observed to increase with pressure between 1 and 15 bar and plateau at higher pressures, which may suggest that these secondary reactions follow a Langmuir-Hinshelwood-type rate equation.

To summarize, during coal pyrolysis pressure plays an indirect role in favouring the cross-linking reactions of free radical fragments by inhibiting the evaporation rate of large aromatic structures. Furthermore, pressure promotes the secondary liquid phase reactions (in the metaplast) by maximizing the residence time of the depolymerized fragments in this phase.

3.2. *Co-pyrolysis of torrefied biomass and coal: effect of pressure*

3.2.1. *On grouped and individual product trends*

The effect of pressure on the yields of grouped products (solid, gas, water and oil) during co-pyrolysis of a 50 wt% blend of torrefied biomass and coal is shown in Fig. 11. The results for the 25 wt% and 75 wt% blends are shown in the Supplementary Data (Table S11 and S13). In general, an increase in pressure resulted in a decrease in the oil yields, from 5.7 to 2.2 wt% at 600 °C (Fig. 11d), and an increase in the gas and pyrolytic water yields, from 17.6 to 23.2 wt% and 11.3–12.6 wt %, respectively (Fig. 11b-c).

The gas release rates during co-pyrolysis of the 50 wt% blend (Fig. 12) showed two stages of gas release: a first stage between 300 and 400 °C where decarbonylation, decarboxylation and demethylation reactions released CO, CO_2 and CH_4 and a second stage at 400–600 °C where all four major gases were released. The pressure significantly affected the release rates of the different gases by promoting the decarbonylation, decarboxylation and demethylation reactions, similar to the results of the pyrolysis of the individual feedstocks (Section 3.1). However, at higher pressures a clear decrease in the release rate of H_2 was observed in the second stage (400–600 °C), which may suggest the promotion of intermolecular hydrogen transfer reactions in the intermediate molten phase during co-pyrolysis (further details in Section 3.2.3). Furthermore, the changes in the composition of oil derived during co-pyrolysis of torrefied biomass and coal were confirmed by the variations in the yields of phenol, methoxyphenol and acid groups (Fig. 13). The pressure mainly affected the yields of acids and phenols. At 600 °C, an increase from 1 to 30 bar resulted in a significant increase in phenol (+4.2 wt%) and acid (+3.2 wt%) groups whereas the change in methoxyphenol yields was insignificant, suggesting the inhibition of demethoxylation reactions during co-pyrolysis (further details in Section 3.2.3).

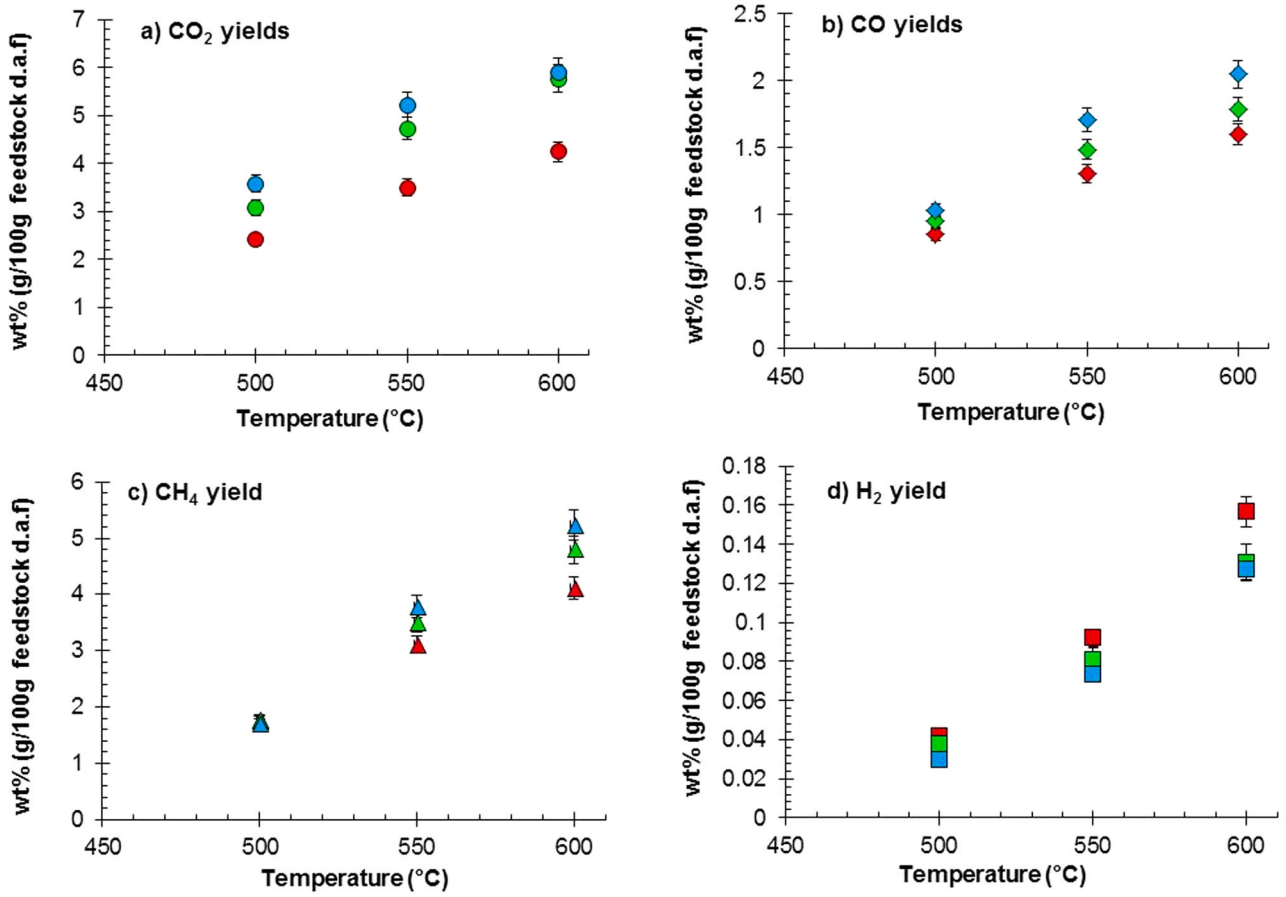

Fig. 8. The effect of pyrolysis pressure and temperature on a) CO_2 yields (● 1 bar), (● 15 bar), (● 30 bar), b) CO yields (◆ 1 bar), (◆ 15 bar), (◆ 30 bar), c) CH_4 yields (▲ 1 bar), (▲ 15 bar), (▲ 30 bar) and d) H_2 yields (■ 1 bar), (■ 15 bar), (■ 30 bar) of coal.

3.2.2. On deviations from additive predictions

The percentage deviation from an additive combination of the single feedstocks is shown in Fig. 14 at different blending ratios and pressures for the main co-pyrolysis products (char, gas, pyrolytic water, and oil). For the 50 wt% blend, higher oil yields and lower water yields were produced during co-pyrolysis at high pressures, which suggests that synergistic interactions were more significant when equal amounts of feedstocks were used. The negative deviation in water yields demonstrates that dehydration and condensation reactions of depolymerized fragments were supressed during co-pyrolysis in favour of synergistic reactions between these fragments. Furthermore, the pressure played a significant role in increasing the extent of these reactions, which may also be observed from the deviation in the oil composition for the different blends (Fig. 15).

Significant deviations were observed for acids (>50%), furanics (>40%), methoxyphenols (>54%) and phenol (>20%) yields (Fig. 15). From these deviations, it was clear that the synergistic reactions between torrefied biomass and coal during co-pyrolysis promoted the release of lignin-derived components (methoxyphenols) and light oxygenates such as acids and furanics, whereas the formation of phenols was inhibited. The presence of coal and its released vapours therefore counteracted the positive effect of pressure on phenol yield in the case of torrefied biomass pyrolysis; changing the reaction selectivity towards 5 C products (such as furanics) and limiting the demethoxylation of 6 C products. In the case of the 50 and 75 wt% blends, the deviation percentage increased at higher pressures for the different groups. The secondary breakdown of oligomers in the liquid intermediate is promoted at high pressures due to the effect of pressure on the evaporation rate of the molten product (as discussed in Section 3.3.1). In the case of co-pyrolysis, a decrease in the evaporation rate of the liquid intermediate at high pressures increased the residence time of the depolymerized fragments (from both feedstocks) in the liquid phase; therefore, the extent of synergistic reactions between the fragments of these two feedstocks increased. These results suggest that the synergistic reactions between torrefied biomass and coal occurred predominately in the intermediate liquid phase, further proven by the absence of any significant change in deviation percentages when the flow rate of the sweep gas was doubled (Supplementary Data Figs. S4 and S5). Further details on the pathways of these synergistic reactions are provided in Section 3.2.2.

3.2.3. On synergistic reactions

3.2.3.1. In the presence of inherent inorganics. The catalytic effect of inherent inorganics (primary inorganics) during pyrolysis significantly alters the product distribution (Fig. 15) [52]. During co-pyrolysis, the blending of coal and torrefied biomass leads to changes in the overall composition of inorganics present in the feedstock matrix (Table 1) and certainly the types and extent of catalytic interactions during depolymerization. For example, the minerals content of torrefied biomass/coal ratio changed from 1:7–1:10–1:17 for the respective blends of 75, 50 and 25 wt%. In the case of co-pyrolysis of torrefied biomass and coal, a clear trend was observed for the promotion of lignin-derived methoxyphenols as well as light oxygenates such as acids, ketones and furanics in the presence of coal. As shown in Fig. 14, a significant positive deviation in the yield of these groups was evident at 25 wt% torrefied biomass blending ratio (12.8 wt% ash); a deviation that became less significant

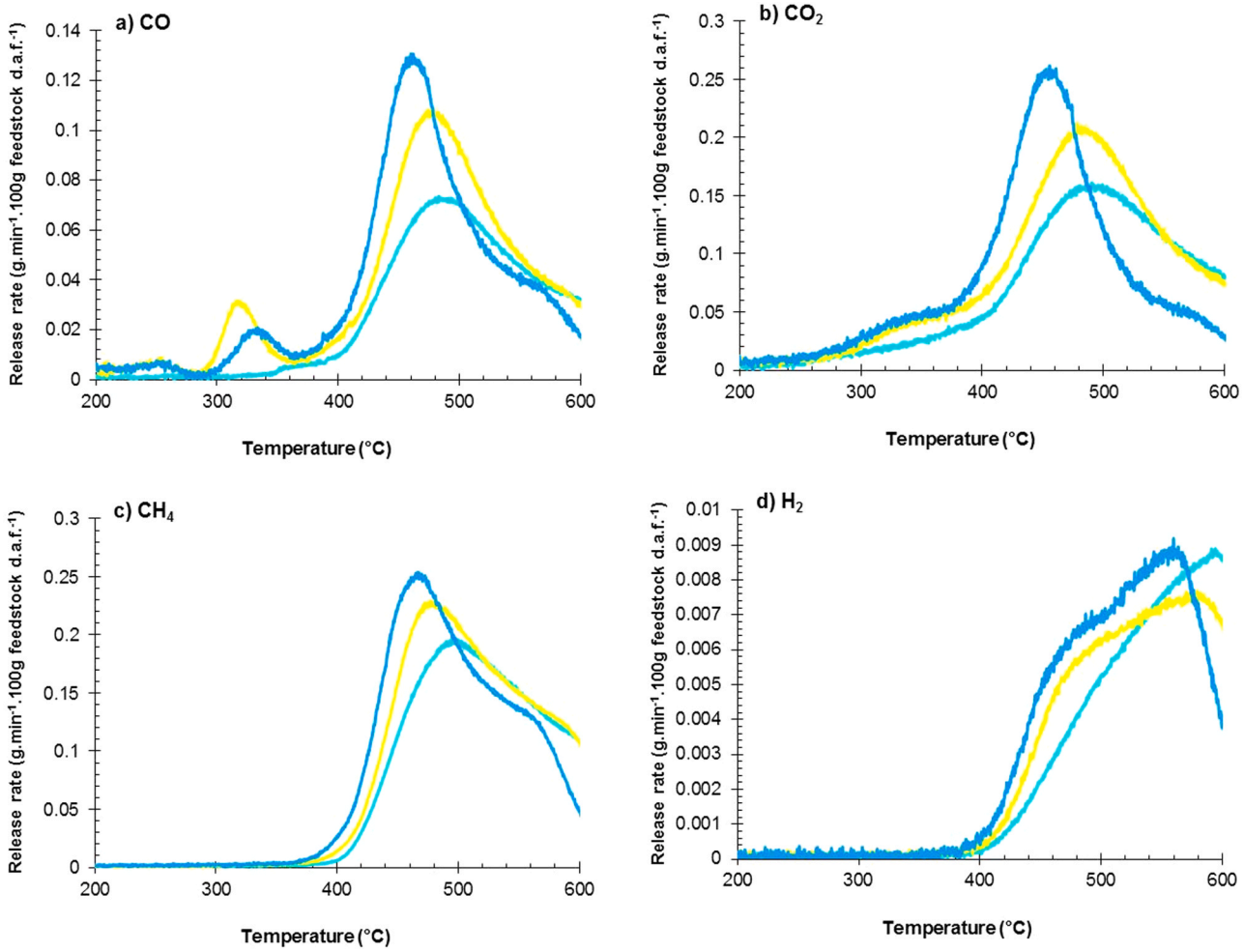

Fig. 9. The release rate of a) CO, b) CO_2, c) CH_4 and d) H_2 during pyrolysis of coal at pressures of 1 bar (—), 15 bar (—) and 30 bar (—).

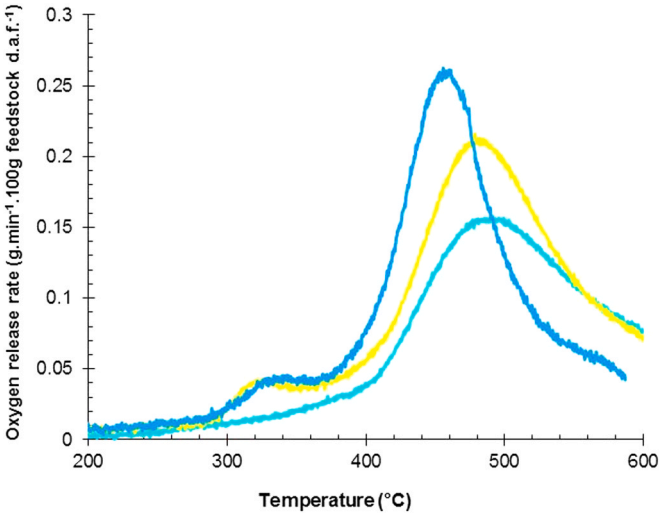

Fig. 10. The oxygen release rate during pyrolysis of coal at pressures at pressures of 1 bar (—), 15 bar (—) and 30 bar (—).

for the 50 wt% (9.2 wt% ash) and 75 wt% (5.6 wt% ash) blends. These results demonstrate the important catalytic role of inherent inorganics during co-pyrolysis.

A comparison of the torrefied biomass and coal ash composition (Table 1) reveals that compared to torrefied biomass, coal contains significantly higher amounts of metallic species such as Al and Ti (3.5 times and 6 times the amount in torrefied biomass, respectively). These metallic species play an important catalytic role as active sites on the surface of the coal, thereby facilitating heterogeneous secondary reactions [5]. These reactions may take place in the molten phase when a small oligomer comes into contact with the active site on the coal surface or in the gas phase via the adsorption of a vaporized molecule onto the surface-active site (Fig. 16). The pressure affects the extent of both reactions: In the molten phase, an increase in pressure decreases the evaporation rate and therefore increases the contact time between a dissolved oligomer and an active site, whereas in the gas phase the surface adsorption of a vaporized molecule onto an active site is enhanced. Therefore, pressure plays an important role in controlling the extent of catalytic interactions between torrefied biomass and coal during co-pyrolysis.

3.2.3.2. In the presence of thermodynamic and chemical interplay. The substantial decrease of the molecular hydrogen production at higher pressures (Fig. 15) is a strong indication that the redistribution of internal hydrogen and/or the extent of hydrogen transfer are enhanced. The stabilization of coal free radical fragments by hydrogen donors from biomass is one of the main mechanisms invoked by studies on co-pyrolysis of raw biomass and coal to explain the suppression of

Table 3
Oil composition (wt% of dry oil) of main chemical families produced during pyrolysis of coal at different temperatures and pressures.

	1 bar			15 bar			30 bar		
	500 °C	550 °C	600 °C	500 °C	550 °C	600 °C	500 °C	550 °C	600 °C
Phenolics[a]	38.7	30.2	29.8	43.2	45.3	46.6	49.1	48.2	53.6
BTX[a]	3.2	3.8	2.5	4.1	2.9	2.6	4.3	2.8	3.0
PAH's[a]	1.5	2.6	2.3	1.7	2.6	2.5	1.4	1.2	1.6
GC-undetected	56.6	63.4	65.4	51.0	49.2	48.3	45.2	47.8	41.8
Phenolics/BTX	12.2	8.0	12.0	10.6	15.4	17.6	11.4	17.3	17.8

[a] Yields of the individual components are provided in the Supplementary Data (Table S10)

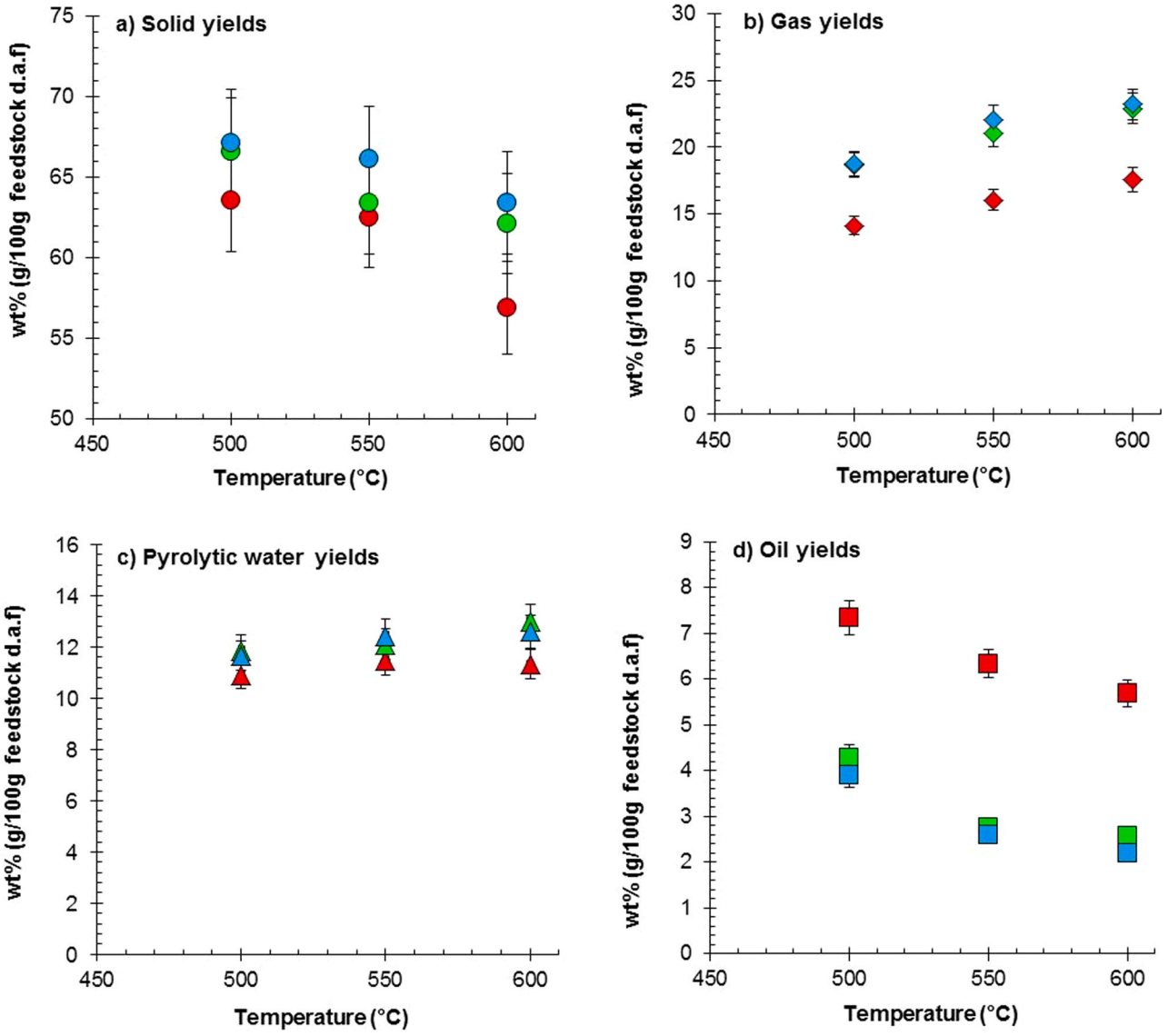

Fig. 11. The effect of pyrolysis pressure and temperature on a) solid residue yields (● 1 bar), (● 15 bar), (● 30 bar), b) gas yields (◆ 1 bar), (◆ 15 bar), (◆ 30 bar), c) pyrolytic water yields (▲ 1 bar), (▲ 15 bar), (▲ 30 bar) and d) oil yields (■ 1 bar), (■ 15 bar), (■ 30 bar) of 50 wt% blend of torrefied biomass and coal.

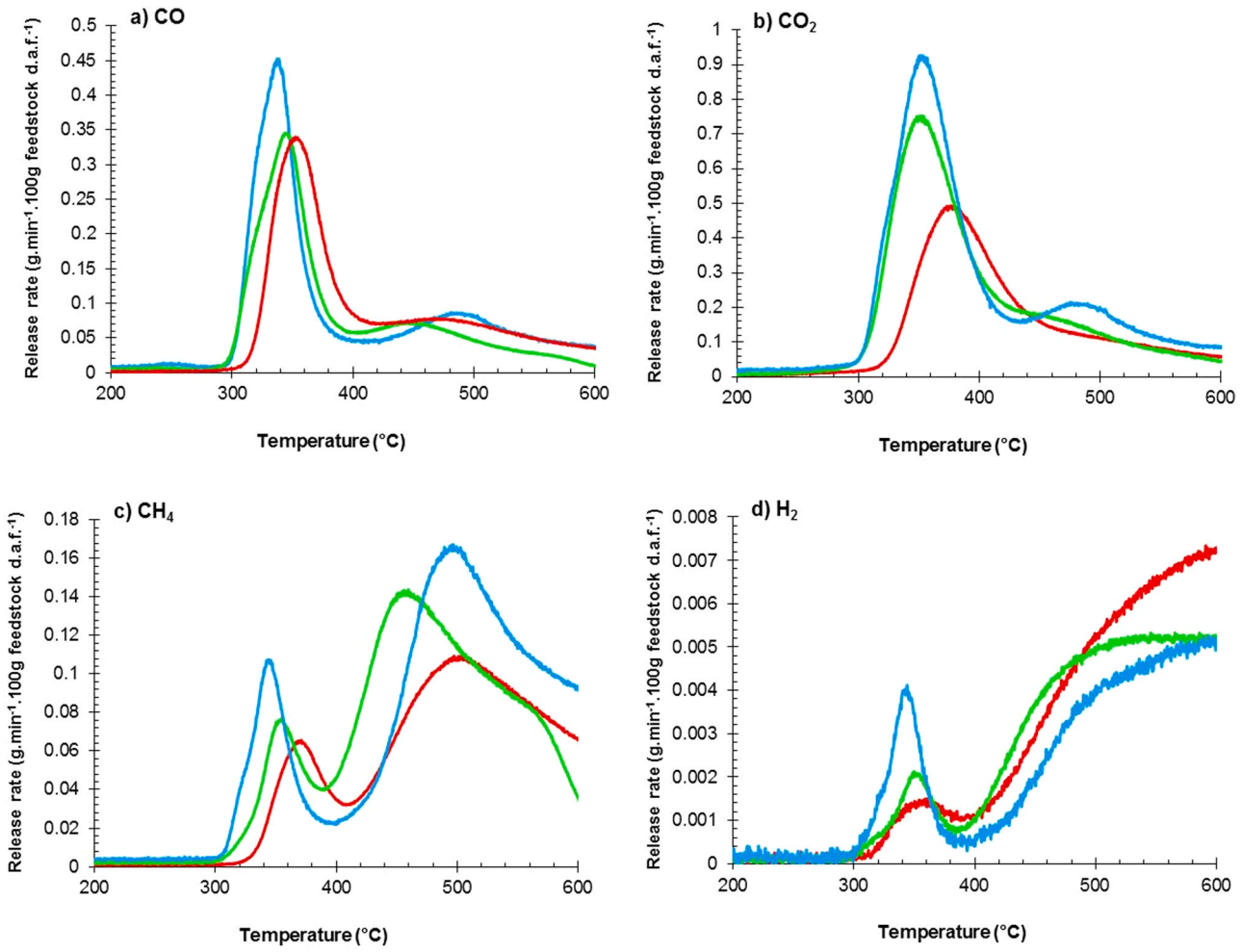

Fig. 12. The release rate of a) CO, b) CO_2, c) CH_4 and d) H_2 during pyrolysis of 50 wt% blend of torrefied biomass and coal at pressures of 1 bar (—), 15 bar (—) and 30 bar (—).

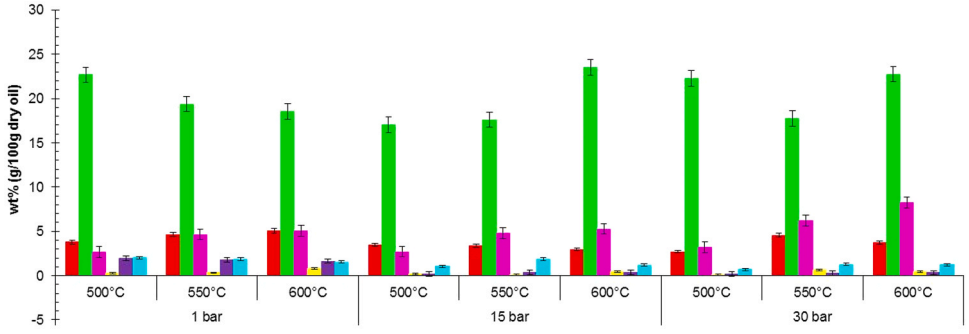

Fig. 13. Yields of methoxyphenols (■), phenols (■), acids (■), ketones (■) anhydrous sugars (■) and furanics (■) during pyrolysis of 50 wt% blend of torrefied biomass and coal at pressures of 1, 15 and 30 bar.

crosslinking and the acceleration of hydrogen transfer [53]. In the case of co-pyrolysis of torrefied biomass and coal, the hemicelluloses have been pre-removed (Table 2). As a result, the presence of torrefied biomass will likely exhibit an improved thermoplastic behaviour during pyrolysis, with a lower O/C ratio (limiting the powerful crosslinking role of oxygen); but will also maximize the potential external hydrogen transfer from cellulose/lignin-derived products to depolymerized coal fragments. Furthermore, the redistribution of hydrogen within the torrefied biomass/coal molten phase can involve both intra- and inter-hydrogen transfer mechanisms, where intra-hydrogen transfer may occur due to backbiting reactions leading to branching of the polymer backbone, whereas inter-hydrogen transfer occurs via abstraction followed by random and unzipping scission reactions [25].

From the results of this study, the most obvious conclusion is that the chemical impact of the presence of a molten phase at higher pressures is more prominent with substantial changes in product distribution. The

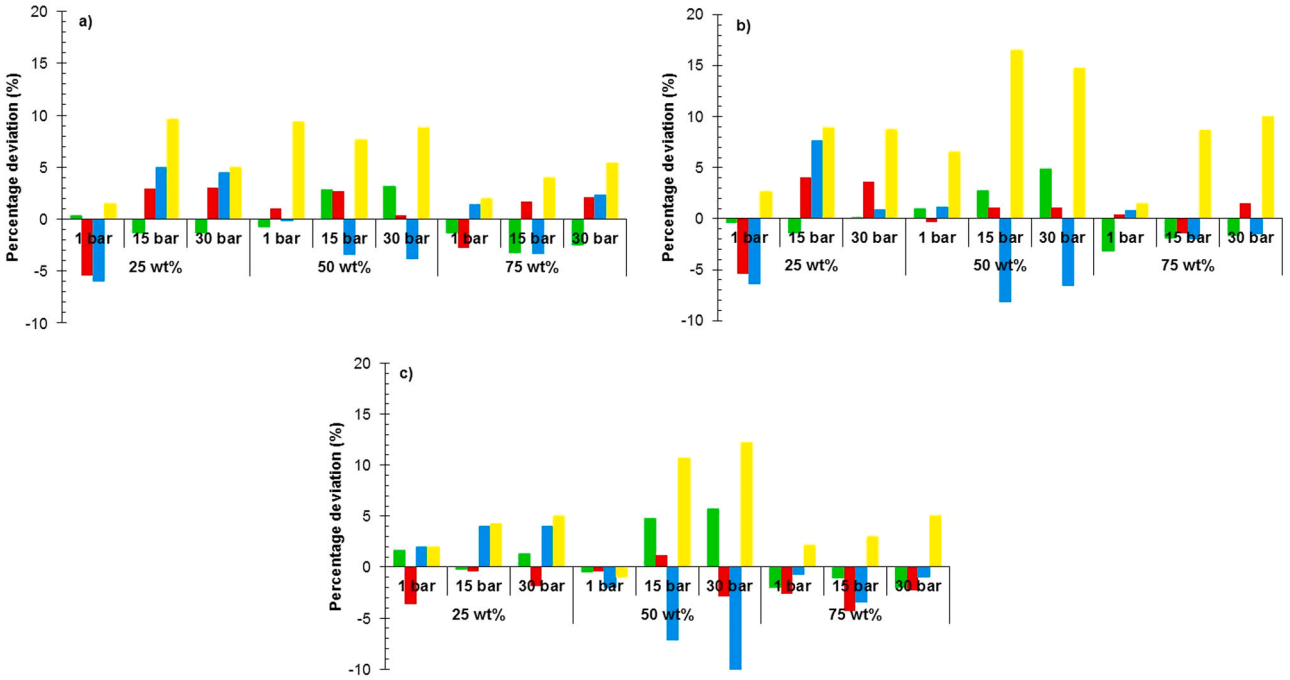

Fig. 14. Percentage deviation from additive model for co-pyrolysis products: Char (■), gas (■), pyrolytic water (■) and oil (■) at pressures of 1, 15 and 30 bar and blending ratios of 25 wt%, 50 wt% and 75 wt% at a) 500 °C, b) 550 °C and c) 600 °C.

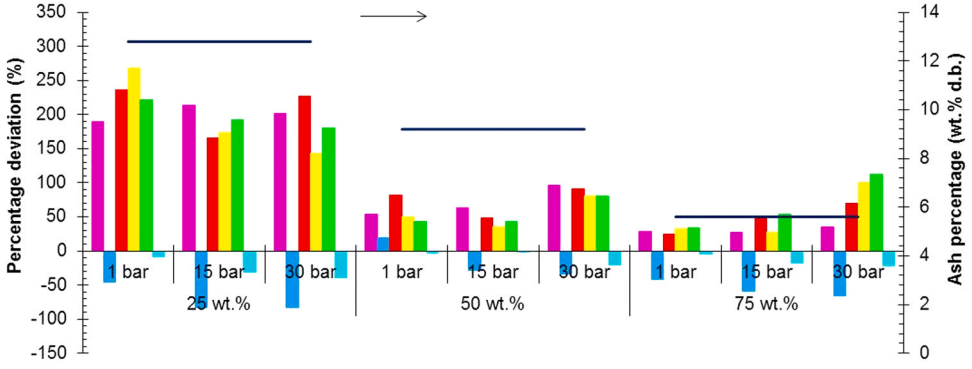

Fig. 15. Ash percentage of different blends (−) and percentage deviation from additive model for methoxyphenol (■), phenols (■), acids (■), ketones (■), furanics (■) and hydrogen (■) yields during co-pyrolysis at 1, 15 and 30 bar.

methoxyphenols yields are significantly enhanced during co-pyrolysis (Fig. 15), whereas the phenol yields show a negative deviation (more significant at high pressures), suggesting the inhibition of demethoxylation reactions in the presence of coal depolymerized fragments. The dissolved coal fragments can increase the density of the molten phase limiting the diffusion of reactive species. The escape of free radicals from the torrefied biomass matrix being prevented, the number of inter-hydrogen transfer reactions in the liquid-phase can be promoted in the case of co-pyrolysis (Fig. 16). Furthermore, pressure controls the evaporation rate and therefore promotes these liquid-phase chemical reactions instead of gas-phase reactions, changing reaction selectivity: demethoxylation reactions being inhibited (possibly prevented by the stabilization of the guaiacol via intra/extra H transfer). Indeed, it has been suggested that the removal of methoxy groups is promoted in the gas phase through a homolytic fission of the O-C bonds [33], which is inhibited during co-pyrolysis. Therefore, the synergistic/antagonistic effects observed during co-pyrolysis are enhanced at high pressures.

4. Conclusion

In this paper, the effect of pressure on the secondary- and synergistic reaction pathways during co-pyrolysis of torrefied biomass and coal was investigated. First, the separate pyrolysis behaviour of both torrefied biomass and coal feedstocks revealed that pressure affected the pyrolysis chemistry: (1) by favouring repolymerization reaction pathways against volatilization pathways at high pressures for both feedstocks, (2) by changing reaction selectivity with the intensification of demethoxylation for torrefied biomass and (3) by promoting the secondary gas/liquid phase reactions for coal.

Based on the additive approach, the effect of pressure and blending degree on the co-pyrolysis of torrefied biomass and coal was assessed. For each blend, the pressure showed to be a significant controlling factor

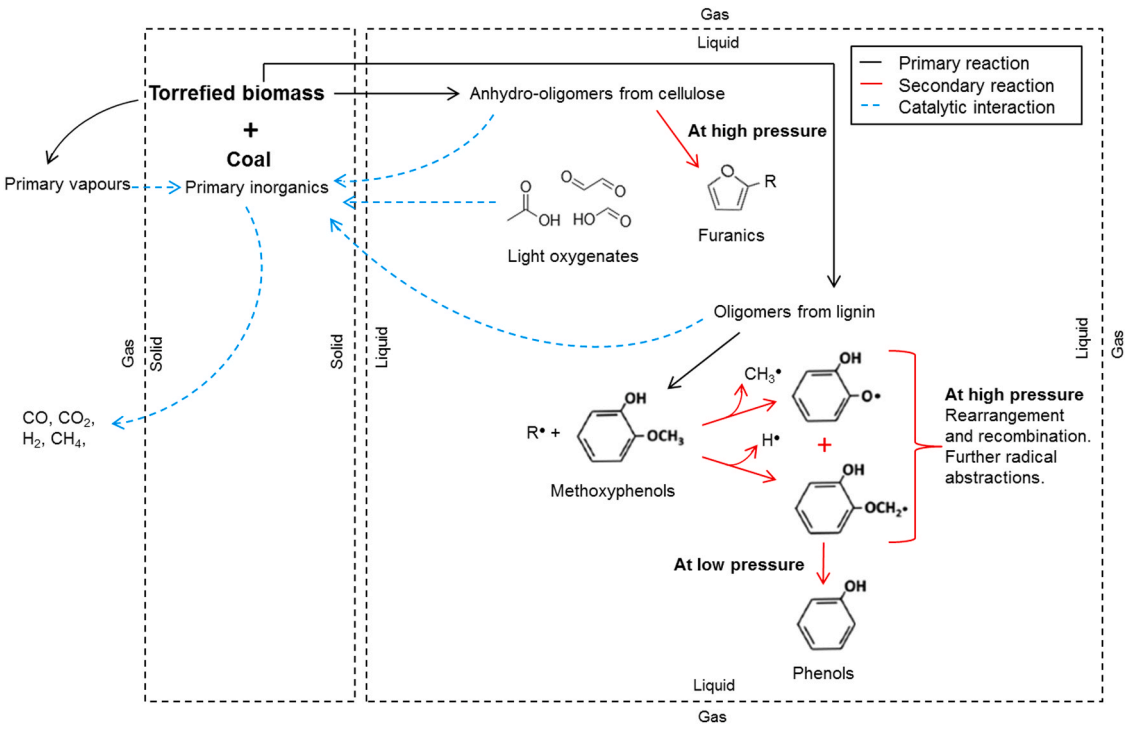

Fig. 16. Proposed synergistic reaction pathways at low temperatures (400–600 °C) adapted from Mettler et al. [24].

to promote reaction selectivity changes with, for example, the bio-oil's chemical composition: increasing the production of acids, furanics and methoxyphenols whereas decreasing phenol formation. The extent of the role of pressure on chemical composition changes was more significant for low blending ratios of torrefied biomass/coal.

The use of higher torrefied biomass/coal ratios significantly decreased the levels and nature of inherent inorganics, which enhanced the role of pressure on the distribution of lumped products by modifying the original competitive reactional balance between devolatilization and repolymerization. Two main events are proposed: (1) the pressure influences the rate of evaporation of the molten phase by limiting it and thereby favouring secondary rearrangement/recombination in the liquid phase; (2) the pressure enhances the surface adsorption of reactants on surface catalytic sites (primary inorganics) and the extent of solid/liquid and solid/gas free radical reactions leading to the formation of secondary char/light oxygenates. The impact of this interplay between the thermodynamic and catalytic effects depends on the blending ratios and therefore on the quantity of molten phase, which controls the propensity of homogeneous and solid/liquid and/or solid/vapour heterogeneous reactions. Further research on synergistic reactions is recommended in the pressure range of 1–15 bar, where the most significant effects of pressure were observed.

CRediT authorship contribution statement

Saartjie M. Gouws: Conceptualization, Methodology, Investigation, Writing – original draft. **Marion Carrier:** Conceptualization, Writing – review & editing. **John R. Bunt**: Supervision, Writing – review & editing. **Hein W.J.P. Neomagus:** Supervision, Writing – review & editing.

Declaration of Competing Interest

The authors declare that they have no known competing financial interests or personal relationships that could have appeared to influence the work reported in this paper.

Acknowledgements

This work was financially supported by the National Research Foundation (NRF) [Coal Research Chair Grant No. 86880] and Sasol. Opinions, findings and conclusions or recommendations expressed in any publication generated by the NRF supported research are that of the author(s) alone, and that the NRF accepts no liability whatsoever in this regard.

Appendix A. Supporting information

Supplementary data associated with this article can be found in the online version at doi:10.1016/j.jaap.2021.105363.

References

[1] M. Patel, X. Zhang, A. Kumar, Techno-economic and life cycle assessment on lignocellulosic biomass thermochemical conversion technologies: a review, Renew. Sustain. Energy Rev. 53 (2016) 1486–1499.

[2] Z. Yang, Y. Wu, Z. Zhang, H. Li, X. Li, R.I. Egorov, P.A. Strizhak, X. Gao, Recent advances in co-thermochemical conversions of biomass with fossil fuels focusing on the synergistic effects, Renew. Sustain. Energy Rev. 103 (2019) 384–398.

[3] G. Perkins, T. Bhaskar, M. Konarova, Process development status of fast pyrolysis technologies for the manufacture of renewable transport fuels from biomass, Renew. Sustain. Energy Rev. 90 (2018) 292–315.

[4] B. Ru, S. Wang, G. Dai, L. Zhang, Effect of torrefaction on biomass physicochemical characteristics and the resulting pyrolysis behavior, Energy Fuels 29 (9) (2015) 5865–5874.

[5] S.M. Gouws, M. Carrier, J.R. Bunt, H.W.J.P. Neomagus, Co-pyrolysis of coal and raw/torrefied biomass: a review on chemistry, kinetics and implementation, Renew. Sustain. Energy Rev. 135 (2021), 110189.

[6] F. Abnisa, W.M.A.W. Daud, A review on co-pyrolysis of biomass: an optional technique to obtain a high-grade pyrolysis oil, Energy Convers. Manage. 87 (2014) 71–85.

[7] A. Bridgwater, G. Peacocke, Fast pyrolysis processes for biomass, Renew. Sustain. Energy Rev. 4 (1) (2000) 1–73.

[8] J. Bunt, F. Waanders, Identification of the reaction zones occurring in a commercial-scale Sasol–Lurgi FBDB gasifier, Fuel 87 (10) (2008) 1814–1823.

[9] J. Van Dyk, M. Keyser, M. Coertzen, Syngas production from South African coal sources using Sasol–Lurgi gasifiers, Int. J. Coal Geol. 65 (3–4) (2006) 243–253.

[10] Y. Huang, N. Waang, Q. Liu, W. Wang, X. Ma, Co-pyrolysis of bituminous coal and biomass in a pressured fluidized bed, Chin. J. Chem. Eng. 27 (7) (2019) 1666–1673.

[11] S. Li, X. Chen, A. Liu, L. Wang, G. Yu, Study on co-pyrolysis characteristics of rice straw and Shenfu bituminous coal blends in a fixed bed reactor, Bioresour. Technol. 155 (2014) 252–257.
[12] Y. Song, A. Tahmasebi, J. Yu, Co-pyrolysis of pine sawdust and lignite in a thermogravimetric analyzer and a fixed-bed reactor, Bioresour. Technol. 174 (2014) 204–211.
[13] S. Li, X. Chen, L. Wang, A. Liu, G. Yu, Co-pyrolysis behaviors of saw dust and Shenfu coal in drop tube furnace and fixed bed reactor, Bioresour. Technol. 148 (2013) 24–29.
[14] H. Zhao, Q. Song, S. Liu, Y. Li, X. Wang, X. Shu, Study on catalytic co-pyrolysis of physical mixture/staged pyrolysis characteristics of lignite and straw over an catalytic beds of char and its mechanism, Energy Convers. Manage. 161 (2018) 13–26.
[15] A.O. Aboyade, M. Carrier, E.L. Meyer, H. Knoetze, J.F. Görgens, Slow and pressurized co-pyrolysis of coal and agricultural residues, Energy Convers. Manage. 65 (2013) 198–207.
[16] A. Collot, Y. Zhuo, D. Dugwell, R. Kandiyoti, Co-pyrolysis and co-gasification of coal and biomass in bench-scale fixed-bed and fluidised bed reactors, Fuel 78 (6) (1999) 667–679.
[17] J.R. Jones, Q. Chen, G.D. Ripberger, Secondary reactions and the heat of pyrolysis of wood, Energy Technol. 8 (6) (2020) 1–13.
[18] E. Hoekstra, R.J. Westerhof, W. Brilman, W.P. Van Swaaij, S.R. Kersten, K. J. Hogendoorn, M. Windt, Heterogeneous and homogeneous reactions of pyrolysis vapors from pine wood, AIChE J. 58 (9) (2012) 2830–2842.
[19] P. Ahuja, S. Kumar, P.C. Singh, A model for primary and heterogeneous secondary reactions of wood pyrolysis, Chem. Eng. Technol.: Ind. Chem.-Plant Equip.-Process Engineering-Biotechnol. 19 (3) (1996) 272–282.
[20] P. Morf, P. Hasler, T. Nussbaumer, Mechanisms and kinetics of homogeneous secondary reactions of tar from continuous pyrolysis of wood chips, Fuel 81 (7) (2002) 843–853.
[21] As Anca-Couce, A. Dieguez-Alonso, N. Zobel, A. Berger, N. Kienzl, F. Behrendt, Influence of heterogeneous secondary reactions during slow pyrolysis on char oxidation reactivity of woody biomass, Energy Fuels 31 (3) (2017) 2335–2344.
[22] Q. He, Q. Guo, K. Umeki, L. Ding, F. Wang, G. Yu, Soot formation during biomass gasification: a critical review, Renew. Sustain. Energy Rev. 139 (2021), 110710.
[23] M.L. Boroson, J.B. Howard, J.P. Longwell, W.A. Peters, Product yields and kinetics from the vapor phase cracking of wood pyrolysis tars, AIChE J. 35 (1) (1989) 120–128.
[24] M.S. Mettler, A.D. Paulsen, D.G. Vlachos, P.J. Dauenhauer, Pyrolytic conversion of cellulose to fuels: levoglucosan deoxygenation via elimination and cyclization within molten biomass, Energy Environ. Sci. 5 (7) (2012) 7864–7868.
[25] D.F. McMillen, R. Malhotra, Hydrogen transfer in the formation and destruction of retrograde products in coal conversion, J. Phys. Chem. A 110 (21) (2006) 6757–6770.
[26] M. Van der Stelt, H. Gerhauser, J. Kiel, K. Ptasinski, Biomass upgrading by torrefaction for the production of biofuels: a review, Biomass Bioenergy 35 (9) (2011) 3748–3762.
[27] A. Boateng, C. Mullen, Fast pyrolysis of biomass thermally pretreated by torrefaction, J. Anal. Appl. Pyrol. 100 (2013) 95–102.
[28] M.J. Prins, K.J. Ptasinski, F.J. Janssen, More efficient biomass gasification via torrefaction, Energy 31 (15) (2006) 3458–3470.
[29] J.S. Tumuluru, S. Sokhansanj, J.R. Hess, C.T. Wright, R.D. Boardman, A review on biomass torrefaction process and product properties for energy applications, Ind. Biotechnol. 7 (5) (2011) 384–401.
[30] L.D. Mafu, H.W. Neomagus, R.C. Everson, M. Carrier, C.A. Strydom, J.R. Bunt, Structural and chemical modifications of typical South African biomasses during torrefaction, Bioresource Technol. 202 (2016) 192–197.
[31] A. Wafiq, D. Reichel, M. Hanafy, Pressure influence on pyrolysis product properties of raw and torrefied Miscanthus: role of particle structure, Fuel 179 (2016) 156–167.
[32] P.R. Solomon, M.A. Serio, E.M. Suuberg, Coal pyrolysis: experiments, kinetic rates and mechanisms, Progr. Energy Combust. Sci. 18 (2) (1992) 133–220.
[33] F.-X. Collard, J. Blin, A review on pyrolysis of biomass constituents: mechanisms and composition of the products obtained from the conversion of cellulose, hemicelluloses and lignin, Renew. Sustain. Energy Rev. 38 (2014) 594–608.
[34] K. Venkatesan, F. Prashanth, V. Kaushik, H. Choudhari, D. Mehta, R. Vinu, Evaluation of pressure and temperature effects on hydropyrolysis of pine sawdust: pyrolysate composition and kinetics studies, React. Chem. Eng. 5 (8) (2020) 1484–1500.
[35] J. Wannapeera, B. Fungtammasan, N. Worasuwannarak, Effects of temperature and holding time during torrefaction on the pyrolysis behaviors of woody biomass, J. Anal. Appl. Pyrol. 92 (1) (2011) 99–105.
[36] D. Shen. The Pyrolytic MechaD. Shen The Pyrolytic Mechanism of the Main Components in Woody Biomass and Their Interactions 2011 University of Southampton.Components in Woody Biomass and Their Interactions, University of Southampton, 2011.
[37] G. Lyu, S. Wu, H. Zhang, Estimation and comparison of bio-oil components from different pyrolysis conditions, Front. Energy Res. 3 (2015) 1–11.
[38] M. Carrier, M. Windt, B. Ziegler, J. Appelt, B. Saake, D. Meier, A. Bridgwater, Quantitative insights into the fast pyrolysis of extracted cellulose, hemicelluloses, and lignin, ChemSusChem 10 (16) (2017) 3212–3224.
[39] S. Konsomboon, J.-M. Commandre, S. Fukuda, Torrefaction of various biomass feedstocks and its impact on the reduction of tar produced during pyrolysis, Energy Fuels 33 (4) (2019) 3257–3266.
[40] W. Cai, Q. Liu, D. Shen, J. Wang, Py-GC/MS analysis on product distribution of two-staged biomass pyrolysis, J. Anal. Appl. Pyrol. 138 (2019) 62–69.
[41] T. Hosoya, H. Kawamoto, S. Saka, Different pyrolytic pathways of levoglucosan in vapor-and liquid/solid-phases, J. Anal. Appl. Pyrol. 83 (1) (2008) 64–70.
[42] T. Hosoya, H. Kawamoto, S. Saka, Solid/liquid-and vapor-phase interactions between cellulose-and lignin-derived pyrolysis products, J. Anal. Appl. Pyrol. 85 (1–2) (2009) 237–246.
[43] J. Montoya, B. Pecha, F.C. Janna, M. Garcia-Perez, Single particle model for biomass pyrolysis with bubble formation dynamics inside the liquid intermediate and its contribution to aerosol formation by thermal ejection, J. Anal. Appl. Pyrol. 124 (2017) 204–218.
[44] B.B. Hattingh, R.C. Everson, H.W. Neomagus, J.R. Bunt, Assessing the catalytic effect of coal ash constituents on the CO_2 gasification rate of high ash, South African coal, Fuel Process. Technol. 92 (10) (2011) 2048–2054.
[45] K.L. Smith, L.D. Smoot, T.H. Fletcher, R.J. Pugmire, The Structure and Reaction Processes of Coal, Springer Science & Business Media, 2013.
[46] P.R. Solomon, D.G. Hamblen, R. Carangelo, M. Serio, G. Deshpande, General model of coal devolatilization, Energy Fuels 2 (4) (1988) 405–422.
[47] P.R. Solomon, M.A. Serio, G.V. Despande, E. Kroo, Cross-linking reactions during coal conversion, Energy Fuels 4 (1) (1990) 42–54.
[48] S. Sommariva, T. Maffei, G. Migliavacca, T. Faravelli, E. Ranzi, A predictive multi-step kinetic model of coal devolatilization, Fuel 89 (2) (2010) 318–328.
[49] P. Wang, L. Jin, J. Liu, S. Zhu, H. Hu, Analysis of coal tar derived from pyrolysis at different atmospheres, Fuel 104 (2013) 14–21.
[50] K. Luo, C. Zhang, S. Zhu, Y. Bai, F. Li, Tar formation during coal pyrolysis under N2 and CO_2 atmospheres at elevated pressures, J. Anal. Appl. Pyrol. 118 (2016) 130–135.
[51] X. Gong, Z. Wang, S. Deng, S. Li, W. Song, W. Lin, Impact of the temperature, pressure, and particle size on tar composition from pyrolysis of three ranks of Chinese coals, Energy Fuels 28 (8) (2014) 4942–4948.
[52] M.S. Mettler, D.G. Vlachos, P.J. Dauenhauer, Top ten fundamental challenges of biomass pyrolysis for biofuels, Energy Environ. Sci. 5 (7) (2012) 7797–7809.
[53] Y. An, A. Tahmasebi, J. Yu, Mechanism of synergy effect during microwave co-pyrolysis of biomass and lignite, J. Anal. Appl. Pyrol. 128 (2017) 75–82.